American Journal of Materials Synthesis and Processing
2019; 4(1): 23-31
http://www.sciencepublishinggroup.com/j/ajmsp
doi: 10.11648/j.ajmsp.20190401.13
ISSN: 2575-2154 (Print); ISSN: 2575-1530 (Online)

Fabrication of AA6061-T6/Al_2O_3 Reinforced Nanocomposite Using Friction Stir Welding

Tanvir Singh*, Shalabh Kumar Tiwari, Dinesh Kumar Shukla

Department of Mechanical Engineering, DR. Bhimrao Ramji Ambedkar National Institute of Technology, Jalandhar, India

Email address:
tanvirsingh3@gmail.com (T. Singh)

*Corresponding author

To cite this article:
Tanvir Singh, Shalabh Kumar Tiwari, Dinesh Kumar Shukla. Fabrication of AA6061-T6/Al_2O_3 Reinforced Nanocomposite Using Friction Stir Welding. *American Journal of Materials Synthesis and Processing.* Vol. 4, No. 1, 2019, pp. 23-31. doi: 10.11648/j.ajmsp.20190401.13

Received: May 24, 2019; **Accepted**: June 25, 2019; **Published**: July 9, 2019

Abstract: In the present work, attempts were made to join AA6061-T6 sheets by Friction Stir Welding (FSW) process. Al_2O_3 nanoparticles were added into the aluminum matrix for refining the microstructure of the nugget zone (NZ) and to restrict the growth of granularly in the heat-affected zone (HAZ). In order to illustrate the influence of Al_2O_3 nanoparticles on mechanical properties, namely ultimate tensile strength, micro-hardness distribution, and wear resistance of the welded joints, FSW was conducted with and without nanoparticles at a constant rotating velocity of 2000 rpm and transverse velocity of 70 mm/min. For characterization of microstructures, optical and scanning electron microscopes were employed. The findings revealed that Al_2O_3 nanoparticles addition along the joint line resulted in remarkable refining of grains structure in the weld nugget zone. This was due to the pinning effect produced by nano-sized Al_2O_3 particles which prevent the grain growth followed by recrystallization during FSW, leading to a remarkable reduction in grain size. Also, the sample with nanoparticles joined at rotating and transverse velocities of 2000 rpm and 70 mm/min showed higher tensile properties than the sample without nanoparticles. However, the employment of single FSW pass resulted in an unusual Al_2O_3 nanoparticles distribution and void initiation at the interface between Al-matrix and Al_2O_3 nanoparticles in the heat-affected zone resulted in the early fracture of welded joints during tensile loading. Moreover, Al_2O_3 nanoparticles addition results in the reduction of frictional coefficient and increment in wear resistance due to fine small grains size and large distribution of hardness in NZ of friction stir welded specimens.

Keywords: FSW, AA6061-T6, Nanocomposites, Microstructural Evolution, Mechanical Characteristics, Reinforced Nanoparticles, Wear Behavior

1. Introduction

Nowadays, weight reduction and less fuel consumption are the two most important demands in the marine, aerospace, and automobile industries. In order to fulfill such demands, soft and light metals as Al-alloys are the most suitable [1-2]. Heat treatable Al-alloys especially AA6061-T6 was most commonly employed in marine frames, pipelines, aircraft, and construction, etc., due to their high corrosive resistance, an extremely large rate of material strength to weight ratio, and ability of weld [3-4].

The most serious concern in regards to joining of aluminum alloys, if conventional fusion welding process (CFWP) was adopted, is their weakening mechanism in the joint area. This was attributed to barriers which come across during (CFWP) of Al-metals, e.g., solidification cracking, porosity/gas interruption, and occurrence of intermetallic brittle phases, etc. Thus, for joining thin aluminum alloys (CFWP) was not acceptable [5-6]. The friction stir welding (FSW) is the most appropriate process to weld aluminum alloy in their solid state [7]. FSW is more capable of joining both like/dislike aluminum metals and alloys [8-11]. In contrast, no melting occurs in FSW in comparison to fusion welding. Because of this reason, this process resolves the issues regarding CFWP [6]. In FSW, localized heat is produced via localized friction occurred at tool and base metal interface and in turn, the mechanical force is applied that results in severe plastic deformation. Also, the amount of generated heat was strongly affected by processing conditions, which could be limited by rotational and traveling

velocities. By keeping all parameters constant, the enhanced heating intensity is acquired by raising the rotating velocity or reducing the transverse velocity. Increase in heating intensity results in a more uniform plasticized flow of material adjacent to the surface of tool which results in wider weld nugget zone and vice-versa [7, 11].

A number of contributions were tested for producing the metal matrix composites (MMC) via FSP [12-14]. In their works, attempts were made by the researchers for fabricating layers on the composite surface of parent metal in which no weldment of parent material took place via friction stir processing. Again, taking into consideration that the FSP passes had a direct impact on the distribution of nanoparticles, while increment in FSP passes lead to the uniform dispersion of nanoparticles [15-16]. However, the influence of transverse and rotational velocities on nanoparticles dispersion and properties (mechanical) of nanocomposites produced via. FSP was reported by numerous researchers. Ezatpour et al. [17] fabricated 6061/Al_2O_3 nanocomposite via. FSP and conclude that the size of grains is decreased by an increment in both traveling and rotating speeds. Saeidi et al. [18] used Al_2O_3 nanoparticles during FSW of 5083/7075 aluminum sheets. They embedded nanoparticles in the joint area and reported the consequences of these nanoparticles on microstructure and toughness behavior of the weldments. The results reveal that Al_2O_3 nanoparticles were uniformly distributed in nugget zone for single FSW pass and comprise of smaller grain size when compared with unreinforced welds. Nikoo et al. [19] incorporated Al_2O_3 nanoparticles on the faying portion of parent alloy during FSW of AA6061 nanocomposites. Their studies indicated three important findings: first, an appreciable enhancement in the properties (especially mechanical) of weldments was noticed due to the addition of nanoparticles in the nugget zone; second, it was noticed that for samples welded at lower traveling speed, severe agglomeration of nanoparticles occurred; third, excellent bonding between Al_2O_3 nanoparticles and AA6061 matrix occurred for samples welded at higher heat input. Marzoli et al. [20] have used Al_2O_3 nanoparticles during FSW of AA6061/20p aluminum alloy for studying their influence on various mechanical and microstructural characteristics. They reported that stirring action of the tool had a remarkable effect on the shape and distribution of Al_2O_3 nanoparticles. Due to this action, the sharp edges of the bigger nanoparticle broke down to change into round particles and due to this reason, a small number of round particles were present in NZ. Consequently, using efficient rotational and travel velocities the MMC was successfully fabricated. Minak et al. [21] used Al_2O_3 nanoparticles during FSW of AA6061/22p aluminum alloy. They reported the influence of nanoparticles addition on mechanical and microstructural properties and found the structure called onion ring that contains Al_2O_3 nanoparticles–rich and Al_2O_3 nanoparticles–free regions in the nugget zone of FSWed samples and also found an appreciable decrement in grain size from 100µm to 10µm in weld nugget zone. Many attempts were made by the researches to elaborate the study on wear resistance behavior for different composites and their allied materials via FSW and FSP [21-23]. The MMC fabricated in the literature reveals low-frictional coefficient and improved resistance to wear when compared with unreinforced samples. Prado et al. [24-25] conducted the study to investigate the wear resistance of nanocomposites prepared via FSW. Their results reveal that Al_2O_3 nanoparticles significantly improved the wear properties when increasing the number of reinforced nanoparticles in the nugget zone. Defect-free and uniform dispersion of reinforcement particles in single FSW pass is a demanding issue which leads to an asymmetric flow of material [12]. For achieving the uniform dispersion of Al_2O_3 nanoparticles in the aluminum metal, various methods, such as increment in passes and reversing the direction of tool rotation during alternate pass has been tried without much success.

With the dual aim of minimizing the ejection of reinforcement particles from the weld line during the single pass and to ensure that distribution of these nanoparticles is uniform in the nugget welded zone, a novel deposition strategy has been adopted in this work (Figure 1a). The arrangement provides good interfacial bonding and allows vigorous intermixing of reinforcement particles with the base material that leads to increment in property gradient. The objective of the present study was to weld AA6061-T6 sheets and to produce Al-Al_2O_3 nanocomposites simultaneously and to study the impact of adding Al_2O_3 nanoparticles on grains structure and various properties (mechanical) of FSWed aluminum matrix.

2. Materials and Methods

AA6061-T6 thin Al-sheets of thickness 2.5 mm were used for FSW. AA6061-T6 chemical composition was obtained by electro-dispersive X-ray spectroscopy that is given in Table 1.

Table 1. *Chemical composition of AA6061-T6.*

Chemical Composition	Mg	Si	Cu	Mn	Cr	Zn	Ti	Al
Wt.%	0.901	0.615	0.258	0.0454	0.19	0.054	0.0195	Bal

For incorporating the Al_2O_3 nanoparticles in the weld nugget, cylindrical holes of diameter 1.5 mm and depth 3 mm were drilled on abutting edges of base material at an equal distance of 13.33 mm. Total 30 numbers of holes were drilled [15 numbers on each sheet] and filled with 460 mg quantity of Al_2O_3 nanoparticles (Figure 1a).

The Al_2O_3 nanoparticles had a diameter of 15 nm with 99.99% of purity and >30 specific surface area. The tool for FSW had a cylindrical shoulder with diameter 15 mm and pin (cylindrical) of length and diameter of 2.30 mm and 5 mm,

respectively (Figure 1b). FSW was done at a constant rotating speed of 2000 rpm, and transverse speed of 70 mm/min (Figure 1c). The tilt of the tool was taken as 0º, whereas the depth of the plunge was 0.2 mm. The embedded conditions along with the specimen nomenclature are mentioned as 2000-70 (sample with nanoparticles) and 2000-70-w (sample without nanoparticles). Samples underwent etching process for 20 seconds using Keller's reagent in order to reveal microstructure and their allied characteristics. Thereafter, the microstructural evolutions as the well-fractured surface of samples are characterized using optical microscopy (OM: Leica DM 2700M) and scanning electron microscopy (SEM: Jeol-124Nx, Japan). Tensile and wear properties of the weldments were also evaluated. Before preparing samples for tensile test, the upper surface of welds was processed through the machining process for eliminating the rough impressions caused by the shoulder surface. For cutting of tensile test samples (Figure 1d), ASTM-E8M-11 was used. Tensile tests are done using the x-head velocity of 2 mm/min. Micro-hardness testing is done along the central portion of the nugget zone at a distance 1mm below the top surface (Figure 1d), by employing 200g load for a period of 15 seconds. The test for wear was done along the upper portion of welds by employing a pin-on-disk arrangement. Tests were performed with 15 N of normal load along with 142 and 0.07 of rotational (rpm) and sliding velocities (mm/s).

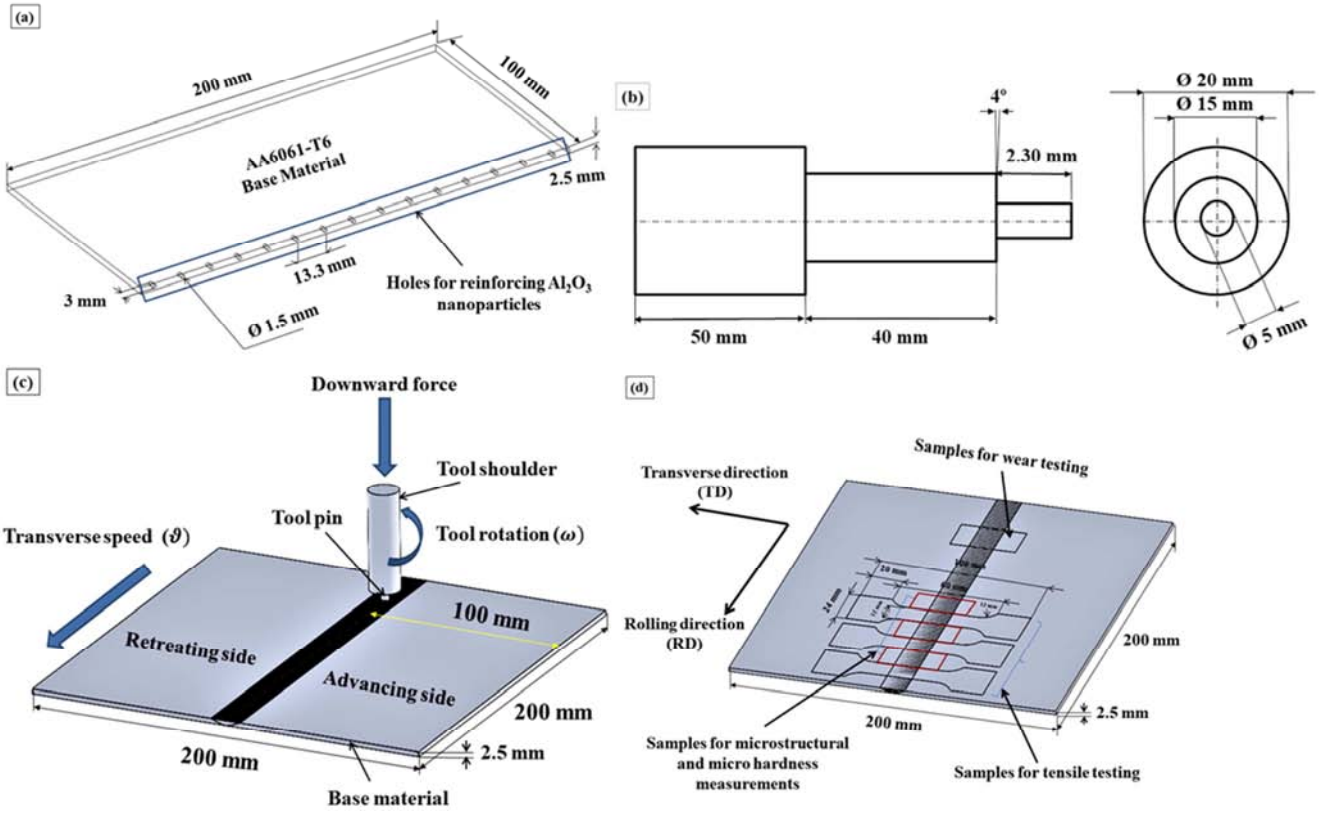

Figure 1. *(a) Representation of nanoparticles reinforced into the aluminum matrix, (b) Design and dimensions of FSW tool, (c) Design of joint and schematic of FSW process, (d) Representation of specimen extracted for various characterization tests.*

3. Results and Discussion

3.1. Macro and Microstructural Characterization

Figure 2 depicts macrographs of with/without nanoparticles samples after the FSW. Higher heating intensity during FSW results in the formation of basin shape nugget zone. It can be noted that the width of the basin in case of the sample without nanoparticle (Figure 2b) is wider than the width of the sample with nanoparticle (Figure 2a). Even though the amount of heat input is same in both the cases, as the Al_2O_3 nanoparticles limit the flow of plasticized material [26].

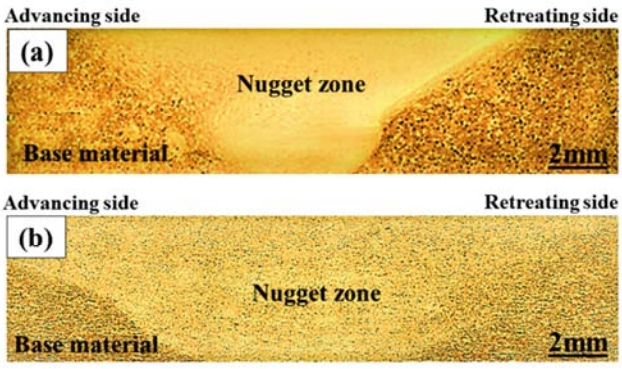

Figure 2. *Cross-sectional macro images of FSWed samples, (a) with nanoparticles, and (b) without nanoparticles.*

Micrographs of (a) base material, FSWed samples (b) Al_2O_3-free and (c) Al_2O_3-included are illustrated in Figure 3. Figure 3a illustrates the micrograph of AA6061-T6 having more elongated grains with average granularly of (38µm), In FSW process, the four zones namely base material (BM), nugget zone (NZ), thermo-mechanical affected zone (TMAZ), and heat affected zone (HAZ) were formed [8, 27-28]. For a sample without nanoparticles, different zones are depicted in Figure 3b. In reference to Figure 3b, base material composed of more elongated grains towards the heat affected zone which does not experience the thermal cycle and induced plastic deformation because of which grains are more similar to the parent metal with an average granularly of (31µm). Whereas, TMAZ experienced partial recrystallization due to which the material is deformed plastically only by the stirring action of the pin that is not sufficient for the dynamic recrystallization to occur as a result the size of grains in the TMAZ is bit bigger (21µm) in comparison to nugget zone and also bent in nature towards the downward flow of the material during the process [6]. But the nugget zone contains fine equiaxed recrystallized grains (18 µm) than the base material (38µm) due to the application of severe plastic deformation and the origin of continuous dynamic recrystallization in the nugget zone [7, 27]. Figure 3c shows the micrograph for a sample with nanoparticles. Micrograph represents the generation of namely two regions as nanoparticle-rich and nanoparticles-free region (more discussed in Figure 4). This was due to the presence of Al_2O_3 nanoparticles that strongly influences the grain size of the NZ. It can be seen that the sample with nanoparticles had a grain size which is considerably (63%) smaller than that of the sample without Al_2O_3 nanoparticles. Thus, incorporating nanoparticles along the weld line gives more fine grains in the nugget zone. This affirms the influence of Al_2O_3 nanoparticles on the refining of the microstructure.

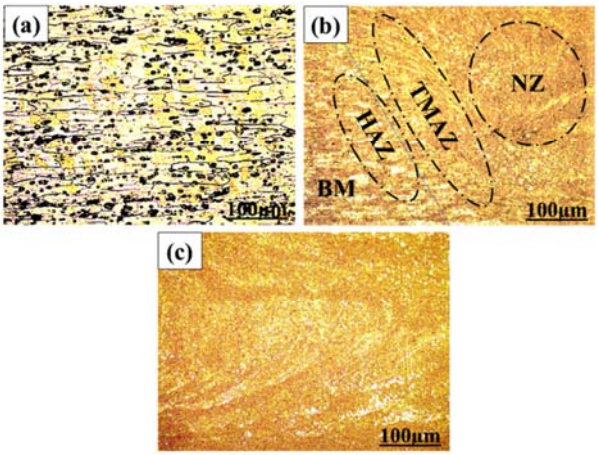

Figure 3. *(a) Representation of microstructures (a) base material before FSW, (b) Different zones occurs in a sample without nanoparticle during FSW, (c) Nugget zone for the sample with nanoparticles.*

Figure 4 presents the optical and SEM photo-images of the NZ for FSWed sample with nanoparticles. According to Figure 4 (a, b), Al_2O_3 nanoparticle-rich and Al_2O_3 nanoparticle-free regions have grain size difference. The mean grain size in NZ for the nanoparticle-rich region (6 µm) was less than the nanoparticle-free region (14µm). Added Al_2O_3 nanoparticles act as the obstruction to the motion of grain boundaries and impede the grain growth via a mechanism called Zener-pinning [5, 29] which influences the dispersion of fine small particles on the migration of high/low angle grain boundaries by exerting pinning force or pressure that contradicts the driving force pushing the grain boundaries. Therefore, the normal growth of the grains is reserved and could not exceed the mean size of grain from a critical radius (R_C) followed by the equation as ($R_C = 4r/3v_f$)[30].

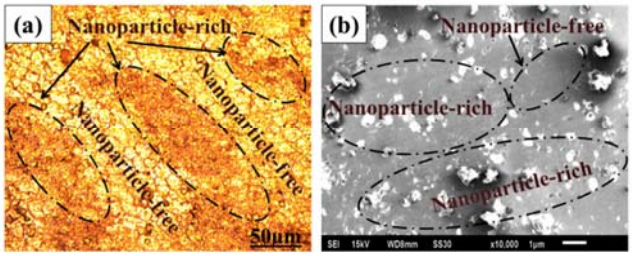

Figure 4. *(a) Optical photo image depicts the dispersion of Al_2O_3 nanoparticles in NZ by forming nanoparticle-rich and nanoparticle-free zones, (b) SEM photomicrographs of Al_2O_3 nanoparticle-rich and Al_2O_3 nanoparticle-free region highlighted in (a).*

Figure 5 represents the optical and SEM photo images taken from agglomerated Al_2O_3 nanoparticles in HAZ for the sample with nanoparticles. In Figure 5a, the Al_2O_3 nanoparticles were agglomerated in the form of flow bands. Figure 5b illustrates the highlighted portion of Figure 5a, in higher magnification. The defects in the form of small cracks are formed adjacent to agglomerated Al_2O_3 nanoparticles because of poor adherence at the interface between nanoparticles and Al-metal. Figure 5c depicts the Si mapping extracted from a portion of Figure 5b, which confirms the presence of agglomerated Al_2O_3 particles in the highlighted area of HAZ. However, a major concern in producing composite reinforced with Al_2O_3 nanoparticles is the distribution of nanoparticles as discussed earlier is dependent on processing parameters.

The addition of Al_2O_3 nanoparticles put significant pinning effect on the migration of grain boundaries, which results in refinement of grains in the NZ. Increasing the rotational speed by keeping welding velocity remain constant it results in creating the large size of the grains in NZ [2, 26, 31]. If, however, the rotational speed is raised again, the amount of generated heat will also increase due to which grains in the NZ will start to evolve [2, 26]. As FSW process is similar to SPD, where the heat generated and rate of strain has an influential effect on the refinement of grains such that dynamic recrystallization (DRX) grains size keep on decreasing by a decrement in the process temperature or increment in the rate of strain [3].

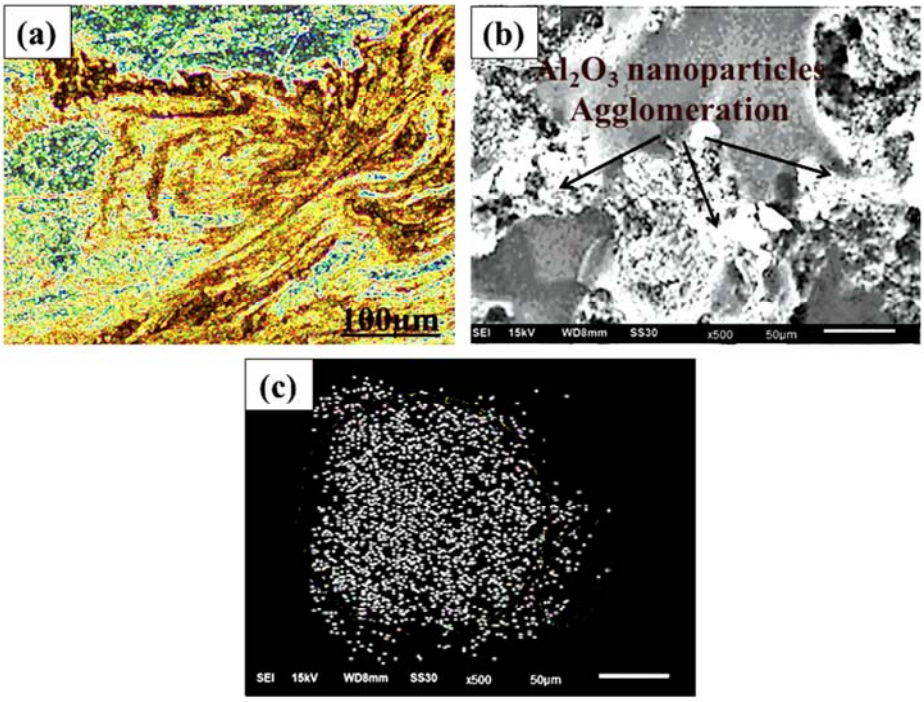

Figure 5. *Optical and SEM photo images of flow bands occurred in HAZ for sample with nanoparticles, (a) Optical image illustrating the nanoparticles accumulated in flow lines, (b) SEM photomicrograph for agglomerated nanoparticle in regions highlighted in (a), (c) Si mapped image of (b) confirms the agglomeration of Al_2O_3 nanoparticles.*

3.2. Microhardness Measurements

Al_2O_3 nanoparticles exhibit a noticeable impact on the micro-hardness variation in NZ. In fact, if the Al_2O_3 nanoparticles are accumulated they behave as most preferable sites for nucleation via the mechanism called particle stimulate nucleation which results in fine small new equiaxed grains after DRX. On the completion of DRX and grain growth stage, individual Al_2O_3 suppress the coarsening of the grains by providing the hindrance to the motion of boundaries of grains and result in fine granularly, i.e., pinning-effect, whereas such reinforcing Al_2O_3 nanoparticles already have a higher distribution of hardness [14] that provides more obstruction to the density of dislocation motion. Hence, the nanocomposites produced in the present study exhibits high strength and hardness. Figure 6 presents the micro-hardness profiles extracted from the NZ of samples with/without nanoparticles.

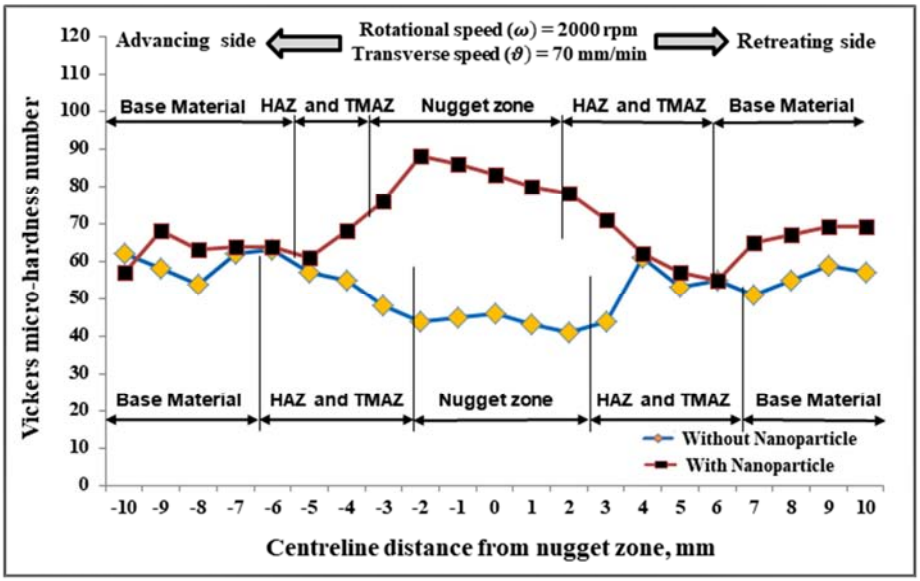

Figure 6. *Microhardness measured transversely from weld centreline for samples with and without Al_2O_3 nanoparticles.*

Clearly, the level of micro-hardness was increased with the addition of Al_2O_3 nanoparticles. It's clear that the sample prepared by using Al_2O_3 nanoparticles had a fine size of grains in comparison with the nanoparticles-free sample. Such fine small equiaxed grains are the reason for more hardenability. Figure 6 reveals some important conclusions as to when Al_2O_3 nanoparticles are incorporated, micro-hardness towards AS is much high in respect to RS. This was due to a higher temperature and less particle velocity occurred on the AS that results in more extrusion and forging of the plasticized material on RS which is extracted and scattered more towards AS [22, 30]. Consequently, with an asymmetrical circulation of plasticized deformed material more distribution of nanoparticles will occur on AS. Whereas for nanoparticles-free FSWed sample, hardness profile exhibit a similar trend on two sides from the nugget zone. The micro-hardness variation in nanoparticles-free sample illustrates consistent hardness distribution in NZ. Such variation in trend on both sides of the nugget zone was increased by adding Al_2O_3 nanoparticles into the Al-matrix.

3.3. Tensile Properties Evaluation

The calculated values of tensile strength for AA6061-T6 and FSW welds are depicted in Figure 7. In accordance with the Figure, FSW samples joined with Al_2O_3 nanoparticles show the highest tensile strength compared to sample without nanoparticles but less than the base material.

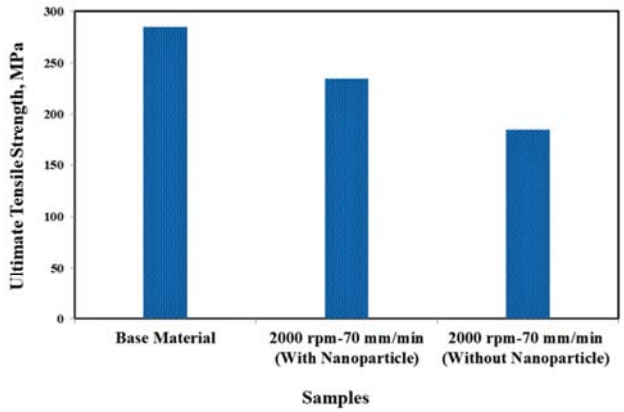

Figure 7. *UTS values for base metal and friction stir welded samples with/without Al_2O_3 nanoparticles.*

These results show the uniform distribution of Al_2O_3 nanoparticles in the nugget zone under these processing parameters. This is because the grain boundaries can pile-up by the Al_2O_3 nanoparticles and as a result prevents the growth of grains. In such cases, smaller grains can lead to strength and hardenability at maximum [30]. When such fine particles interact with the dislocation density, it can lead to two conditions depending upon the nanoparticles' size. Condition-1, if there are small size nanoparticles, the cutting of such nanoparticles is done by dislocation and in turn pile-up leading to strengthening (Orowan strengthening). Condition-2, for large size nanoparticles, the formation of loops will occur, which again the reason for materials strengthening. Figure 8 illustrates the photo images of fracture appearances and fracture locations for the tensile samples with and without nanoparticles and base material. It can be seen that in Figure 8a, the tensile sample for the base material shows ductile failure. For sample without nanoparticles, Figure 8b, failure will occur more towards the base material from the nugget zone showing appreciable ductility. It is clearly depicted in Figure 8c, that for the sample with nanoparticles fracture occurred on the AS from HAZ with no plastic deformation.

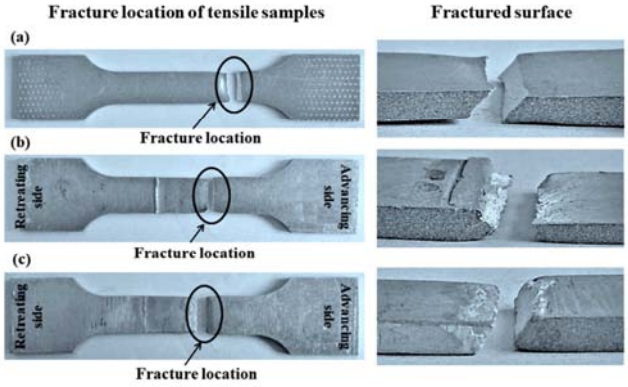

Figure 8. *Cross-sectional photo images of fracture location and the fractured surface of tensile samples (a) base material, (b) without Al_2O_3 nanoparticles, and (c) with Al_2O_3 nanoparticles.*

This is because of the presence of severely agglomerated Al_2O_3 nanoparticles in HAZ [30-32]. Figure 9 presents the SEM photomicrographs of the fractured portion of samples with and without nanoparticles. As depicted in Figure 9a, the Al_2O_3 nanoparticles are densely agglomerated in the HAZ because of which fracture of the sample took place along the above-mentioned region. It is well understood that agglomeration of Al_2O_3 nanoparticles will act as the initial site for nucleating the crack/void at the interface between Al-matrix and Al_2O_3 nanoparticles, which is responsible for lower ductility and sudden premature fracture of the sample. Whereas, for the sample without nanoparticles, the occurrence of deep small dimples indicates the mode of ductile fracture and affirms the improvement in ductility (Figure 9b).

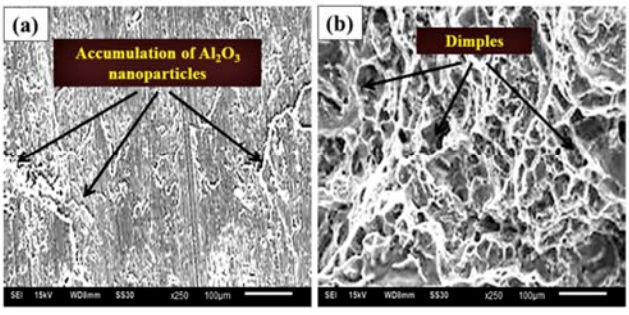

Figure 9. *SEM photomicrographs for the fractured surface of samples (a) with Al_2O_3 nanoparticles, (b) without Al_2O_3 nanoparticles.*

3.4. Wear Testing Measurements

The corresponding results for wear resistance tests are illustrated in Figure 10. The results comprise of weight loss and the frictional coefficient for 2000-70 and 2000-70-w samples compared with the base material (Table-2).

Table 2. *The amount of weight loss after wear test for samples with/without nanoparticles and base material.*

	Weight loss (mg)
Parent material	5.6
2000-70 (With Al_2O_3)	7.5
2000-70 (Without Al_2O_3)	4.1

Furthermore, in the case of 2000-70 samples, the frictional coefficient was substantially less in comparison to the parent metal. It is obvious due to fine small grains size and large distribution of hardness in NZ of friction stir welded specimens. As far as 2000-70 sample is concerned, the frictional coefficient is comparatively less than that of the base metal but higher in comparison with the 2000-70-w sample. This was due to the addition of Al_2O_3 nanoparticles which results in the reduction of frictional coefficient provided that these nanoparticles are distributed uniformly within the aluminum matrix.

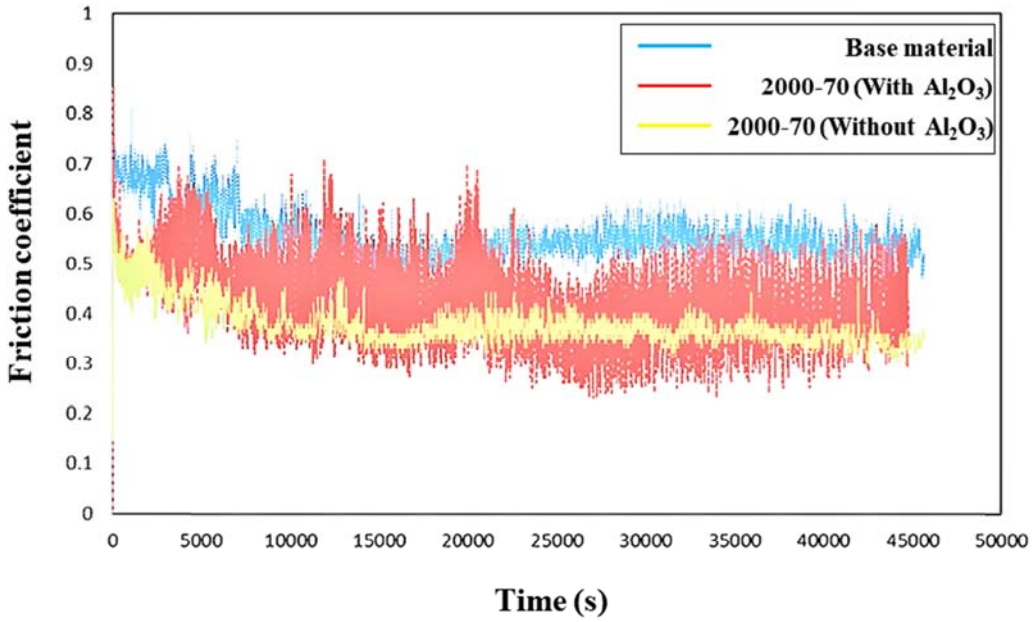

Figure 10. *Frictional coefficient values for the sample with and without Al_2O_3 nanoparticles in comparison with the base material.*

Therefore, with an increase in FSW runs, decrement in the coefficient of friction can be enhanced [32]. This is due to unusual Al_2O_3 nanoparticles distribution which results in nanoparticles agglomeration. For such cases, the poor adhesion between the Al_2O_3 nanoparticles and the Al-metal would occur. So, during wear test for such sample, separation, and overlay of coated surface layering could happen instead of erosion which results in large weight loss compared to parent material and 2000-70-w sample. Based on Figure 10, the high peak amplitude of the frictional trend for this sample can also be the result of non-uniform dispersion of Al_2O_3 nanoparticles in HAZ.

4. Conclusions

The effects of Al_2O_3 nanoparticles addition on microstructural and mechanical characteristics of friction stir welded nanocomposite were studied. It was found that the AA6061-T6/Al_2O_3 nanocomposite can successfully be fabricated through FSW in a single FSW pass at optimal rotating and transverse velocities of 2000 rpm and 70 mm/min. Macrostructural and microstructural studies showed that the amount of high heating intensity during FSW results in a difference in width of the nugget zone as Al_2O_3 nanoparticles limit the flow of plasticized material. However, the incorporation of Al_2O_3 nanoparticles provides substantial influence on the grain refinement in the nugget zone via pinning effect which prevents the grain growth followed by recrystallization during FSW, leading to a significant reduction in grain size. Besides, average grains size was decreased from 38 µm for parent metal to 6 µm for the sample with nanoparticles. Mechanical characteristics reveal that the micro-hardness in NZ for the sample with Al_2O_3 nanoparticles is comparatively higher than sample free-nanoparticle which is due to the existence of strong-ceramic nanoparticles, and their role in reducing the size of the grains via Zener-pinning effect and providing the hindrance to the motion of dislocations. Whereas, the ultimate tensile strength for Al_2O_3 nanoparticles sample is higher than nanoparticle-free sample under the same processing parameters which are mainly due to the refinement of grains and Orowan strengthening mechanism occurred due to fine dispersed nano-sized Al_2O_3 particles. Less resistance to wear with high loss of weight was observed due to unusual Al_2O_3

nanoparticles distribution in the HAZ on the advancing side leads to aggregation of nanoparticles in HAZ and poor bonding between accumulated Al_2O_3 nanoparticles and aluminum matrix which results in overlay/lamination and surface layer separation.

References

[1] F. C. Liu, Z. Y. Ma, "Influence of Tool Dimension and Welding Parameters on Microstructure and Mechanical Properties of Friction-Stir-Welded 6061-T651 Aluminium Alloy," *Metall. Mater. Trans. A*. 39 (10), 2378–2388, 2008.

[2] J. He, Z. Ling, H. Li, "Effect of tool rotational speed on residual stress, microstructure, and tensile properties of friction stir welded 6061-T6 aluminum alloy thick plate," *Int. J. Adv. Manuf. Technol.* 84 (9–12), 1953–1961, 2016.

[3] KAUFMAN JG. Introduction to aluminum alloys and tempers [M]. ASM. Int., 2000.

[4] ASM Handbook. 02, 2004.

[5] M. D. A. Pasha, P. R. Reddy, P. Laxminarayana, I. A. Khan, "SiC and Al_2O_3 Reinforced Friction Stir Welded Joint of Aluminium Alloy 6061," *International Journal of Precision Engineering and Manufacturing-Green Technology*. 5 (1), 151–172, 2018.

[6] T. Prakash, S. Sivasankaran, P. Sasikumar, "Mechanical and Tribological Behaviour of Friction-Stir-Processed Al 6061 Aluminium Sheet Metal Reinforced with Al_2O_3/0.5Gr Al_2O_3/0.5Gr Hybrid Surface Nanocomposite", *Int. J. Adv. Manuf. Technol*. 80 (9–12), 1919–1926, 2015.

[7] R. S. Mishra, M. W. Mahoney, "Friction", 2007.

[8] T Khaled, "An outsider looks at friction stir welding", ANM-112N-05-06, 2005.

[9] S. Yazdanian, Z. W. Chen, G. Littlefair, "Effects of friction stir lap welding parameters on weld features on advancing side and fracture strength of AA6060-T5 welds", *J. Mater. Sci*. 47 (3), 1251–1261, 2012.

[10] Y. S. Sato, M. Urata, H. Kokawa, "Parameters controlling microstructure and hardness during friction-stir welding of precipitation-hard enable aluminum alloy 6063", *Metall. Mater. Trans. A*. 33 (3), 625–635, 2002.

[11] F. J. Liu, L. Fu, H. Y. Chen, "Effect of high rotational speed on temperature distribution, microstructure evolution, and mechanical properties of friction stir welded 6061-T6 thin plate joints", *Int. J. Adv. Manuf. Technol.* 96 (5–8), 1823–1833, 2018.

[12] N. Gangil, S Maheshwari, A. N. Siddiquee, "Multipass FSP on AA 6063-T6 Al: Strategy to fabricate surface composites", *Mater. Manuf. Processes*. 33 (7), 805-811, 2018.

[13] J. Guo, B. Y Lee, Z. Du, G. Bi, M. J. Tan, J Wei, "Effect of Nano-Particle Addition on Grain Structure Evolution of Friction Stir Processed Al 6061 During Post-Weld Annealing", *Arab. J. Sci. Eng.* 40 (2), 559–569, 2015.

[14] C. M. A. Fernández, R. A. Rey, M. J. C. Ortega, D. Verdera, C. L. Vidal, "Friction-stir processing strategies to develop a surface composite layer on AA6061-T6", "*Mater. Manuf. Process*. 33 (10), 1-8, 2018.

[15] M. Sharifitabar, A. Sarani, S. Khorshahian, M. S. Afarani, "Fabrication of 5052Al/Al_2O_3 nanoceramic particle reinforced composite via friction stir processing route", *Mater. Des.* 32, 4164–4172, 2011.

[16] M. Yang, C. Xu, C Wu, K. C. Lin, Y. J. Chao, L. An, "Fabrication of AA6061/Al_2O_3n`ano ceramic particle reinforced composite coating by using friction stir processing", *J. Mater. Sci.* 45, 4431–4438, 2010.

[17] H. R. Ezatpour, S. A. Sajjadi, M. H. Sabzevar, A. Chaichi, G. R. Ebrahimi, "Processing map and microstructure evaluation of AA6061/Al_2O_3 nanocomposite at different temperatures", *Trans. Nonferrous. Met. Soc. China.* 27 (6), 1248-1256, 2017.

[18] M. Saeidi, M. Barmouz, M. K. B. Givi, "Investigation on AA5083/AA7075+Al_2O_3 Joint Fabricated by Friction Stir Welding: Characterizing Microstructure, Corrosion and Toughness Behaviour", *Mater. Res.* 18 (6), 1156-1162, 2015.

[19] M. F. Nikoo, H. Azizi, N. Parvin, H. Y. Naghibi, "The influence of heat treatment on microstructure and wear properties of friction stir welded AA6061-T6/Al_2O_3 nanocomposite joint at four different traveling speed", *J. Manuf. Process.* 22, 90–98, 2016.

[20] L. M. Marzoli, A. V. Strombeck, J. F. D. Santos, C. Gambaro, L. M. Volpone, "Friction stir welding of an AA6061/Al2O3/20p reinforced alloy", *Compos. Sci. Technol.* 66, 363–371, 2006.

[21] G. Minak, L. Ceschini, I. Boromei, M. Ponte, "Fatigue properties of friction stir welded particulate reinforced aluminum matrix composites", *Int. J. Fatigue.* 32, 218–226, 2010.

[22] D. Aruri, K. Adepu, K. Bazavadaa, "Wear and mechanical properties of 6061-T6 aluminum alloy surface hybrid composites [(SiC +Gr) and (SiC + Al_2O_3)] fabricated by friction stir processing", *J. Mater. Res. Technol*. 2 (4), 362–369, 2013.

[23] N. Parumandla, K. Adepu, "Effect of Al_2O_3 and SiCnano-reinforcements on microstructure mechanical and wear properties of surface nanocomposites fabricated by Friction Stir Processing", *Maters. Sci.* 24 (3), 338-344, 2018.

[24] PRADO RA. MURR LE, SHINDO DJ, SOTO KF. Tool wear in the friction-stir welding of aluminum alloy 6061+20% Al2O3: a preliminary study [J]. Scr Mater, 2001, 45: 75-80.

[25] R. A. Prado. L. E. Murr, K. F. Soto, J. C. Mcclure, "Self-optimization in tool wear for friction-stir welding of Al 6061/20% Al_2O_3 MMC", *Mater. Sci. Eng. A.* 349, 156-165, 2003.

[26] C. Sharma, D. K. Dwivedi, P. Kumar, "Effect of welding parameters on microstructure and mechanical properties of friction stir welded joints of AA7039 aluminum alloy", *Mater. Des.* 36, 379–390, 2012.

[27] D. Lohwasser, Z. Chen, "Friction stir welding from basics to applications", 2010.

[28] G. Singh, K. Singh, J. Singh, "Effect of process parameters on microstructure and mechanical properties in friction stir welding of aluminum alloy", *Trans. Indian. Inst. Met.* 64, 325–330, 2011.

[29] O. S. Salih, H. Ou, W. Sun, D. G. Mccartney, "A review of friction stir welding of aluminum matrix composites", *Mater. Des*. 86, 61–71, 2015.

[30] P. Cavaliere, A. D. Santis, F. Panella, A. Squillace, "Effect of welding parameters on mechanical and microstructural properties of dissimilar AA6082–AA2024 joints produced by friction stir welding", *Mater. Des.* 30 (3), 609–616, 2009.

[31] L. Ceschini, I. Boromei, G. Minak, A. Morri, F. Tarterini, "Microstructure, tensile and fatigue properties of AA6061/20 vol. %Al_2O_{3p} friction stir welded joints", *Compos. Part. A.* 38, 1200–1210, 2007.

[32] S. Zarghani, S. F. K. Bozorg, A. Z. Hanzaki, "Microstructures and mechanical properties of Al/Al_2O_3 surface nano-composite layer produced by friction stir processing", *Mater. Sci. Eng. A*. 500, 84–91, 2009.